PHILOSOPHICAL TRANSACTIONS OF THE ROYAL SOCIETY A MATHEMATICAL, PHYSICAL & ENGINEERING SCIENCES

The Stratospheric and Mesospheric Sounder on Nimbus 7

J. R. Drummond, J. T. Houghton, G. D. Peskett, C. D. Rodgers, M. J. Wale, J. Whitney and E. J. Williamson

Phil. Trans. R. Soc. Lond. A 1980 **296**, 219-241
doi: 10.1098/rsta.1980.0166

Phil. Trans. R. Soc. Lond. A **296**, 219–241 (1980) [219]
Printed in Great Britain

The stratospheric and mesospheric sounder on Nimbus 7

By J. R. Drummond, J. T. Houghton, F.R.S., G. D. Peskett, C. D. Rodgers, M. J. Wale, J. Whitney and E. J. Williamson
Department of Atmospheric Physics, Clarendon Laboratory, Oxford, OX1 3PU

The stratospheric and mesospheric sounder (s.a.m.s.) instrument was launched on the Nimbus G satellite on 24 October 1978. It is designed to measure temperature and concentration profiles of various gases in the height range 20–100 km by detecting either their thermal emission or, in some cases, resonant scattering of sunlight.

The gases selected, CO_2, CO, CH_4, NO, N_2O and H_2O, significantly affect the upper atmosphere energy budget by their influence on the concentration of the primary sunlight absorber, ozone. This influence is disproportionate to their own concentration because of the existence of 'catalytic cycles' which destroy ozone while regenerating the catalyst.

A description of the instrument, its principles of operation and some of the methods of retrieval used is presented, together with some preliminary results from the first 3 months of operations.

1. Introduction

As has been explained earlier in this meeting by Professor Labitzke and by Dr Barnett, during the last 10 years remote sounding observations from satellites of atmospheric temperature have been extended through the stratosphere into the mesosphere. Much extra insight into atmospheric phenomena has arisen through the provision of these observations substantially continuous in time and with near global coverage. The purpose of the stratospheric and mesospheric sounder (s.a.m.s.) on Nimbus 7 is to provide similar coverage in time and space for observations of the concentration of a number of important minor constituents in the stratosphere and mesosphere, all of which are directly or indirectly involved in the chemistry of ozone (cf. Thrush, this symposium). Like previous remote sounding instruments built for Nimbus satellites in which the Oxford University Atmospheric Physics Department has been involved, s.a.m.s. observes infrared radiation emitted by the atmospheric constituents it is required to measure. In this paper, the principles of the techniques employed will first be outlined, then the different measurements being made by s.a.m.s. will be discussed together with a description of the instrument and the method of calibration. Finally, some early results will be presented.

2. Principles of operation

2.1. *Limb-sounding*

The advantages of the limb view (see figure 7) are that emission observations can be made from as long a path through the atmosphere as possible, and that behind the atmospheric path is the cold radiation background of space. Such a limb path possesses an air mass approximately 70 times that in a vertical path above the lowest point of the path. The atmosphere's pressure profile and the geometry of the path both weight the material in the path strongly towards the tangent height giving good vertical resolution. For emission from spectral lines that are

not saturated at their centres, 60 % of the emission from a limb path originates from altitudes within 3 km of the lowest altitude of the path (see figure 4). By contrast, the horizontal resolution of a limb observation is poor, the length of the limb path being of the order of 400 km.

Radiometers carried by balloons or aircraft have, for a long time, observed emission from the atmosphere's limb. Results from the limb radiance inversion radiometer (l.r.i.r.) on Nimbus 6 (Gille *et al.* 1975), the first satellite radiometer to observe radiance from the atmosphere's limb, have demonstrated the vertical resolution which can be achieved in measurements of temperature and ozone (Gille, this symposium).

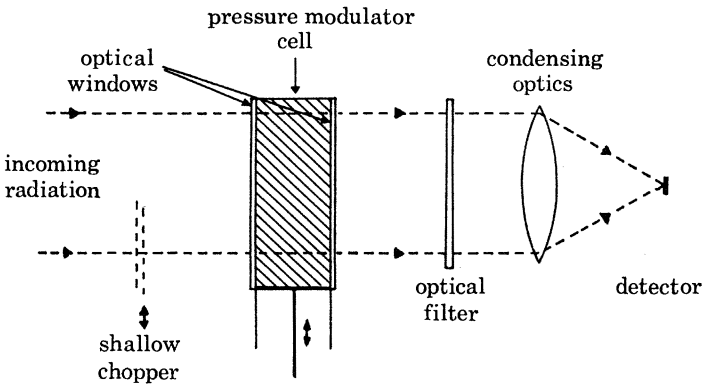

FIGURE 1. Simplified diagram of a p.m.r. optical system employing a 'shallow chopper' which only modulates part of the incoming radiation beam.

2.2. *The pressure modulator*

The pressure modulator is a device which selectively modulates the emission from a gas by using the absorption lines of the same gas as an optical filter. A cell of gas is included in the optical path of the radiometer (figure 1) and its pressure varied cyclically. The transmission of the cell is modulated only at optical frequencies that lie within the absorption lines of the gas, thus selectively modulating emission from the same gas incident on the radiometer. After detection, the signal at the frequency of the modulation may be recovered by phase-sensitive detection. A broad optical filter limits the spectral bandwidth to the appropriate emission band.

The pressure modulator technique is a development from the selective chopper technique employed for temperature sounding instruments on the Nimbus 4 and 5 satellites (Houghton & Smith 1970; Ellis *et al.* 1973). It has previously been flown in a temperature sounder on the Nimbus 6 satellite (Taylor *et al.* 1972; Curtis *et al.* 1974). The advantages of the technique for composition sounding have been described by Chaloner *et al.* (1978), who employed it in a balloon-borne radiometer for the measurement of NO, NO_2 and H_2O in the stratosphere. Further details of the technique are also given in Drummond & Jarnot (1978).

2.3. *Double chopping*

The gas pressure in the pressure modulator cell (p.m.c.) is modulated at the resonant frequency (20–40 Hz) of the mechanical system (see § 4.3). It is also useful to include a conventional chopper at a much higher frequency (*ca.* 240 Hz) in the optical system. This modulates all 'incoming' radiation with the optical filter profile and produces a 'wideband' signal

at the detector. The 'wideband' signal, in the absence of emission from other species, provides information for lower in the atmosphere than the p.m.r. signal (see figure 2). The wideband signal may also be used for the elimination of signals from atmsopheric constituents whose absorption bands overlap that of the wanted species (see Drummond & Jarnot 1978), and in the determination of the atmospheric level being observed (§ 3.3). In s.a.m.s. a shallow chopper is employed (see § 4), which chops only *ca.* 2.5 % of the aperture of the system. The shallow chopper is preferred over a conventional 100 % chopper because it does not obstruct the beam for the pressure modulator further back in the optical chain.

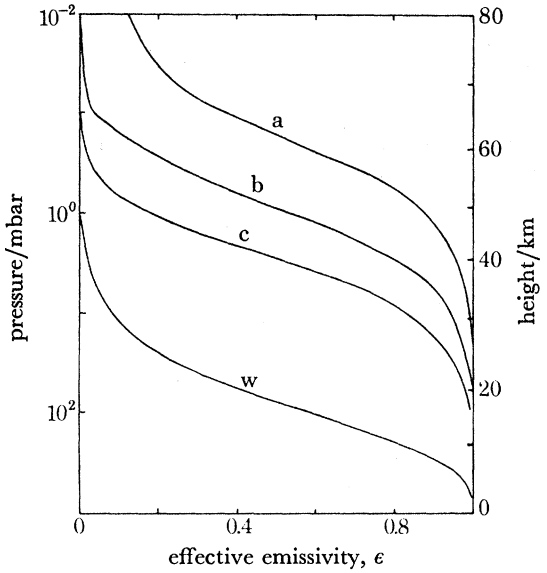

FIGURE 2. The effective emissivity, ϵ (see equation (5)) for water vapour evaluated by using a climatological equatorial temperature profile and a constant volume mixing ratio of 5×10^{-6}. Curves (a), (b) and (c) are for the s.a.m.s. B2 p.m.r. channel with mean cell pressures of 0.87 mbar, 4.48 mbar and 15.3 mbar respectively. Curve (w) is for the corresponding wideband channel and is virtually independent of modulator pressure.

3. MEASUREMENTS WITH S.A.M.S.

The radiant power, W, emitted by a limb path at frequency ν and received by one of the s.a.m.s. detectors is given by

$$W = A\Omega \int_0^\infty \int_0^\infty J_\nu(x)\, \tau_{0\nu}\, \tau_{m\nu}\, \frac{\mathrm{d}\tau_\nu(x)}{\mathrm{d}x}\, \mathrm{d}x\, \mathrm{d}\nu, \tag{1}$$

where A is the aperture of the telescope, Ω the field of view, $\tau_\nu(x)$ the transmission between the satellite and the position along the path described by the coordinate x, $\tau_{0\nu}$ the static component of the optical transmission in the appropriate channel, $\tau_{m\nu}$ the modulated component of the optical transmission, and $J_\nu(x)$ is the source function appropriate to the emission band in question at the location described by the coordinate x. Under conditions of local thermodynamic equilibrium (l.t.e.), the source function is equal to the Planck function $B_\nu(T)$ at the temperature T of the atmosphere at location x.

Integration is along the limb path and over the frequencies where the optical components have any significant transmission.

Calibration of the instrument is carried out by inserting a black-body at temperature T_b in the path when the radiant power W_b received is

$$W_b = A\Omega \int_0^\infty B_\nu(T_b)\, \tau_{0\nu} \tau_{m\nu}\, \mathrm{d}\nu. \tag{2}$$

The radiance, L, of an atmospheric path is then defined as

$$L = \frac{W}{W_b} \frac{\int_0^\infty B_\nu(T_b)\, \tau_{0\nu} \tau_{m\nu}\, \mathrm{d}\nu}{\int_0^\infty \tau_{0\nu} \tau_{m\nu}\, \mathrm{d}\nu}. \tag{3}$$

For channels covering a reasonably narrow frequency interval the ratio of the integrals in equation (3) is $B_{\bar{\nu}}(T_b)$, where $\bar{\nu}$ is the centre frequency of the interval.

To illustrate the radiometric measurements being made it is useful when l.t.e. applies to write a simplified expression for the radiance L measured by a particular channel, namely:

$$L = \epsilon B_{\bar{\nu}}(\overline{T}), \tag{4}$$

where

$$\epsilon = \frac{\int_0^\infty \int_0^\infty \tau_{0\nu} \tau_{m\nu} \frac{\mathrm{d}\tau_\nu(x)}{\mathrm{d}x}\, \mathrm{d}x\, \mathrm{d}\nu}{\int_0^\infty \tau_{0\nu} \tau_{m\nu}\, \mathrm{d}x} \tag{5}$$

may be defined as the *effective emissivity* of the path and where $\overline{T}$ is a mean temperature for the path.

3.1. *Temperature measurements*

If the radiance is measured from the emission band of an atmospheric constituent whose distribution is accurately known, for any given path the emissivity ϵ in equation (4) may be calculated and hence a mean temperature $\overline{T}$ for that path may be deduced. A set of radiances received from different levels as the instrument scans over the limb may be retrieved to give a temperature profile (see Rodgers (1976) for a review of retrieval methods and § 6.2). In s.a.m.s. two wideband and two pressure modulator channels are included observing emission from the 15 μm band of CO_2, a gas that is substantially uniformly mixed up to at least 90 km altitude. Above about 80 km, local thermodynamic equilibrium no longer applies for this band; the quantity that is then measured is the vibrational temperature of the band, which is of considerable importance because emission from it is the major energy sink in the upper mesosphere and lower thermosphere.

3.2. *Composition measurements*

Given that the atmosphere's temperature structure has been determined by the method of § 3.1, from radiance observations on any other band an effective emissivity ϵ may be determined from equation (4), and hence the distribution of the emitting constituent observed. In figure 2 are curves showing the variation of effective emissivity for emission from the long wave water vapour band as measured by a wide band channel and by channels containing pressure modulator cells with water vapour at different pressures, demonstrating that the water vapour distribution can be measured from the tropopause through into the upper mesosphere. Some results for H_2O from an early orbit of s.a.m.a. are given in § 6.

The method by which a detailed distribution is derived is as follows. First of all, through theoretical calculations on the basis of spectral information about the band in question, together with a programme of laboratory measurements as described in § 5, algorithms describing the transmission of any atmospheric path are derived. A 'first guess' profile for the distribution of the gas in question is then assumed and, on the basis of the temperature profile derived by the method of § 3.1, an expected set of radiances is computed. These computed radiances are then compared with the measured radiances, and by an iterative process a profile of the gas distribution is found for which computed and measured radiances agree.

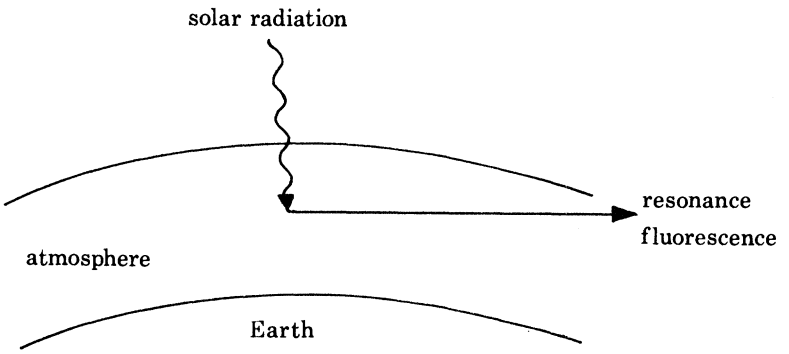

FIGURE 3. The generation of resonance fluorescence signals by scattering of sunlight within the atmosphere.

To acquire information about the distribution of some constituents in the mesosphere and lower thermosphere it is possible to use observations of resonance fluorescence of solar radiation from those molecules which have strong bands in the near infrared (figure 3) (cf. Table 1 for list of bands included in s.a.m.s.). Provided that absorption by solar radiation is the only process of excitation of the band in question, and provided that collisional quenching is negligible, the radiance observed is a function of the solar flux incident on the layer and the number of molecules along the path. In practice, an elaborate radiative transfer calculation has to be carried out for each situation because multiple scattering, excitation by other non-thermal processes (e.g. by particles), and details of quenching processes have also to be considered. Interpretation of measurements from fluorescence channels, therefore, is extremely complex.

3.3. *Reference pressure determination*

Because s.a.m.s. is a limb viewing instrument it is necessary that accurate information is available regarding the pressure of the atmosphere at the levels being viewed at any given time. Consider information such as that contained in figure 2. When, for instance, the effective emissivity of an atmospheric path is about 0.5, a change in signal corresponding to a change in emissivity of 0.01 (equivalent to a change in mixing ratio of *ca.* 6 %) could also result from a change in the level being viewed of 0.15 km, which is equivalent to a change in pressure at the tangent point of *ca.* 2 % or 0.003° in viewing direction.

The attitude of the spacecraft is controlled only to *ca.* 0.5° in all three axes; it is therefore necessary from the measurements made by s.a.m.s. itself to determine the appropriate information about the pressure at the part of the atmosphere being observed.

A method for providing this information arises from comparing the signals from a wideband and a pressure modulator channel in the 15 μm CO_2 band. Under the approximation of equation

(4) the two signals will be $\epsilon_w B(\overline{T}_w)$ and $\epsilon_p B(\overline{T}_p)$ where the subscripts w and p respectively denote the wideband and pressure modulator channels. Now it is possible to choose the mean cell pressure in the pressure modulator channel such that over a certain range of altitudes the relative contributions of different segments of the atmospheric path being observed are very similar for the two channels, even though the effective emissivity of the atmosphere for the two channels is very different (figure 4). This means that $\overline{T}_w$ and $\overline{T}_p$ will be almost equal. We then find that the ratio ϵ_p/ϵ_w is almost independent of temperature but strongly dependent on the pressure at the level of observation. Figure 5 illustrates that, for a particular cell pressure, atmospheric pressure over the range between 0.8 mbar and 20 mbar may be derived from the ratio of signals in the two channels. A first order correction for the atmospheric temperature profile can be included, enabling pressure measurement of adequate accuracy (*ca.* 2 %) to be achieved. In § 6 an example of the use of the method with s.a.m.s. data is presented.

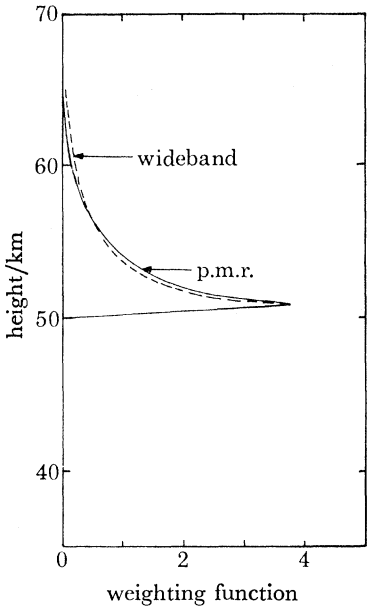

FIGURE 4. A typical pair of CO_2 15 μm weighting functions for the s.a.m.s. attitude-determining channels before the finite field-of-view is accounted for. The tangent height of the line-of-sight is 50 km.

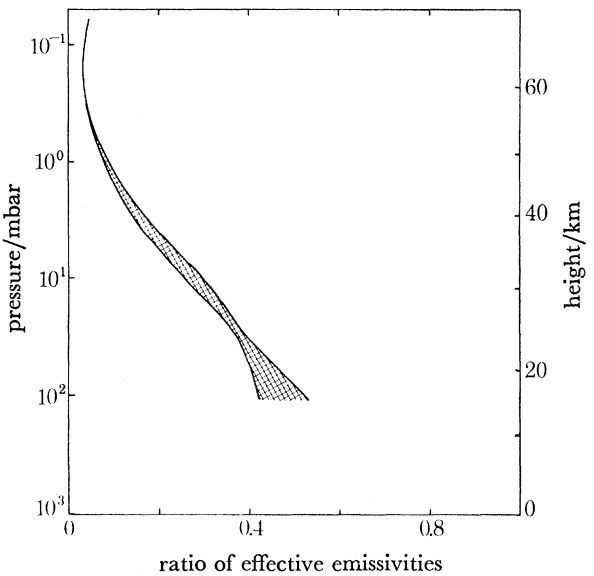

FIGURE 5. Ratio of p.m.r. to wideband emissivities for the 15 μm CO_2 channels C1 at 15 mbar mean cell pressures. The envelope shown is the extreme of a series of curves derived using climatological temperature profiles at 10° latitude intervals from Newell (1977). The effect of the finite instrument field-of-view has also been included in the calculation.

3.4. *Wind determination*

Through the incorporation in the instrument of cells containing the gases whose emission is being detected, the possibility exists of measuring atmospheric motion. If the emitting gas in the atmosphere possesses a significant velocity along the line of sight relative to the gas in the absorbing cells, the emission lines will be shifted relative to the absorbing lines. Figure 6 shows the variation of signal with azimuth angle for a particular case. The direction along which the signal is a maximum is that along which there is zero Doppler shift and hence zero relative velocity of the atmosphere with respect to the spacecraft. If the position of this maximum is

determined, knowing the spacecraft velocity vector, and making allowance for the rotation of the Earth, the wind speed along the line of sight can be found. For directions nearly perpendicular to the spacecraft's velocity vector, a change in azimuth direction of 0.1° introduces *ca.* 10 ms^{-1} of the spacecraft's velocity along the line of sight.

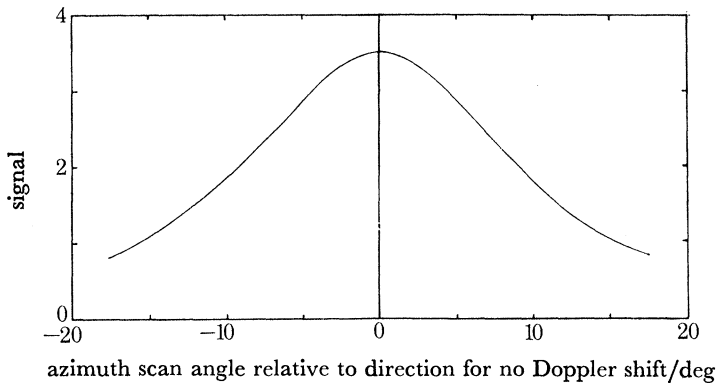

FIGURE 6. Variation of the signal from the 15 μm CO_2 p.m.r. channel with azimuth scan angle relative to the central point where there is no relative motion along the line-of-sight between the atmosphere and the instrument.

So that the influence of atmospheric variations is a minimum, the azimuth scan is carried out at such a rate that during the scan the same part of the atmosphere is kept under observation. A scan over 30° (figure 6) then takes about 240 s. The main problem in carrying out the measurement is that of the maintenance of adequate attitude stability during the period of scan so that the slope of the curve of signal against scan angle is not disturbed by attitude changes. With the Nimbus 7 spacecraft the attitude stability is not adequate for accurate wind determination, although it is hoped that the stability will sometimes be sufficient for the lower mesospheric jet at *ca.* 60 km altitude to be detected.

TABLE 1. S.A.M.S. RADIOMETRIC CHANNELS

field of view	channel	constituent (gas in modulator)	mean cell pressures / mbar	spectral band / μm	derived quantities and altitude range
A	A1	CO_2	17, 2.4, 0.69, 0.25	15	kinetic temperature 15–80 km; attitude
	A2				ν_2 vibrational temperature 80–100 km
	A3	CO	14.8, 4.5	4–5	
	A4	NO	45, 20		distribution 15–60 km
B	B1	H_2O	16, 4.5, 0.8, 0.5	2.7	distribution 80–100 km
	B2			25–100	distribution 15–100 km
C	C1	CO_2	36, 11.2, 3.25, 0.87	15	kinetic temperature 15–80 km; attitude
	C2	N_2O	24.4, 7.15	7.7	distribution 15–60 km
	C3	CH_4	47.8, 22.5		

3.5. *Instrument performance*

S.a.m.s. contains a number of channels for various measurements. Some of these channels may be operated simultaneously and some are mutually exclusive. A list of all channels is shown in table 1. Each entry in the constituent column corresponds to a modulator and each entry in

the spectral band column to a detector. Since it is only possible to pass one pair of signals (p.m.r. and wideband) through a detector at any one time only one modulator signal using a particular detector may be processed at any time. Therefore, only one of the gases N_2O and CH_4 may be measured at a particular time and only one of CO, NO and 4.3 μm CO_2. A detailed description of how the channels are fitted together in the instrument is given in § 4.

TABLE 2. INSTRUMENT PERFORMANCE FOR TEMPERATURE AND COMPOSITION MEASUREMENTS FROM PRESSURE MODULATOR CHANNELS

gas	CO_2	NO	N_2O/CH_4	CO_2	CO_2	H_2O
band/μm	4.3	5.3	7.7	15	15	25–100
altitude of observation/km	120	40	40	50	100	50
approximate integration time for n.e.e. = 0.03† as measured by s.a.m.s. on Nimbus 7 /s	10000	400	10	4‡	2000	5

† n.e.e. = noise equivalent emissivity. An n.e.e. = 0.03 implies a S/N of 33 when instrument observing black body at atmospheric temperature.

‡ n.e.e. = 0.01 as this is a temperature sounding channel required to measure to ±1 K.

It can be seen from figure 2 that over a large part of the sensitive region for composition sounding a 10 % change in composition produces a change of about 3 % in the observed signal. In table 2 some typical integration times required to detect such a change are tabulated for various channels in the instrument at typical heights in the atmosphere.

4. THE S.A.M.S. INSTRUMENT

The s.a.m.s. radiometer instrument consists of two modules: the sensor housing containing the optics, mechanisms and detectors, and a separate electronics module. The overall size of the sensor (see figure 8) is 55 cm × 30 cm × 55 cm and it weighs 23.6 kg. The electronics module weighs 6.7 kg. The average power consumption is about 20 W.

There are a total of twelve radiometric channels: six pressure modulator and six wideband channels distributed between three fields-of-view denoted A, B and C. The relation between the three fields is fixed by the geometry of the instrument optics and is illustrated in figure 7. Some of the channels may be used to sense one of several constituents selected by programmable control logic within the instrument (see § 4.7). Figure 7 also shows the scanning range of the instrument for limb views and space calibration.

4.1. *Optical system*

The optical system may be conveniently subdivided into two sections:

(*a*) the front optics comprising scan mirror, telescope, calibration system and wideband chopper;

(*b*) the rear optics comprising field separator mirror, pressure modulator cells, detectors and optical relay components. The front optics is shown in figure 9. Incident radiation is first reflected from the scanning mirror (M1), which can rotate about two axes for both limb

(vertical) and azimuth (horizontal) scanning (see § 4.5). It is then reflected from the main paraboloid (M2) to the primary focus forming a telescope of 177 cm² area and 22 cm focal length.

During in-flight calibration a small black body is rotated into the beam at the primary focus to give a known input radiance to the rest of the optical system.

After the primary focus the beam is directed by ellipsoid (M3) and plane (M4) mirrors through the fast, shallow chopper (see § 4.4) to the secondary focus at the field separation mirror

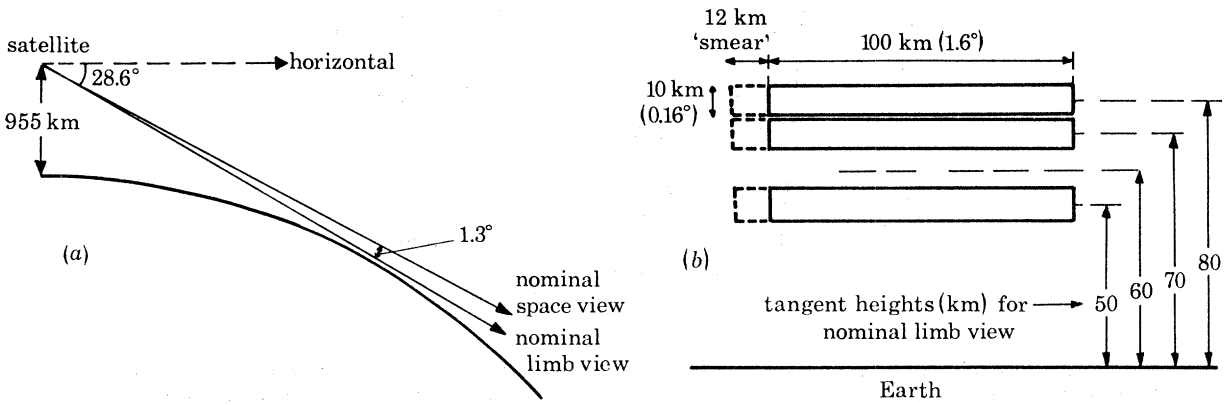

FIGURE 7. (*a*) The geometry of the s.a.m.s. viewing direction. Note that only very small angular moments are necessary to scan the entire atmosphere. As drawn the satellite velocity is into the paper. (*b*) The relative positions of the three fields-of-view A, B and C viewed along the direction of the line of sight in the 'nominal limbview' position. The horizontal smear is caused by spacecraft motion during a 2 s measurement period.

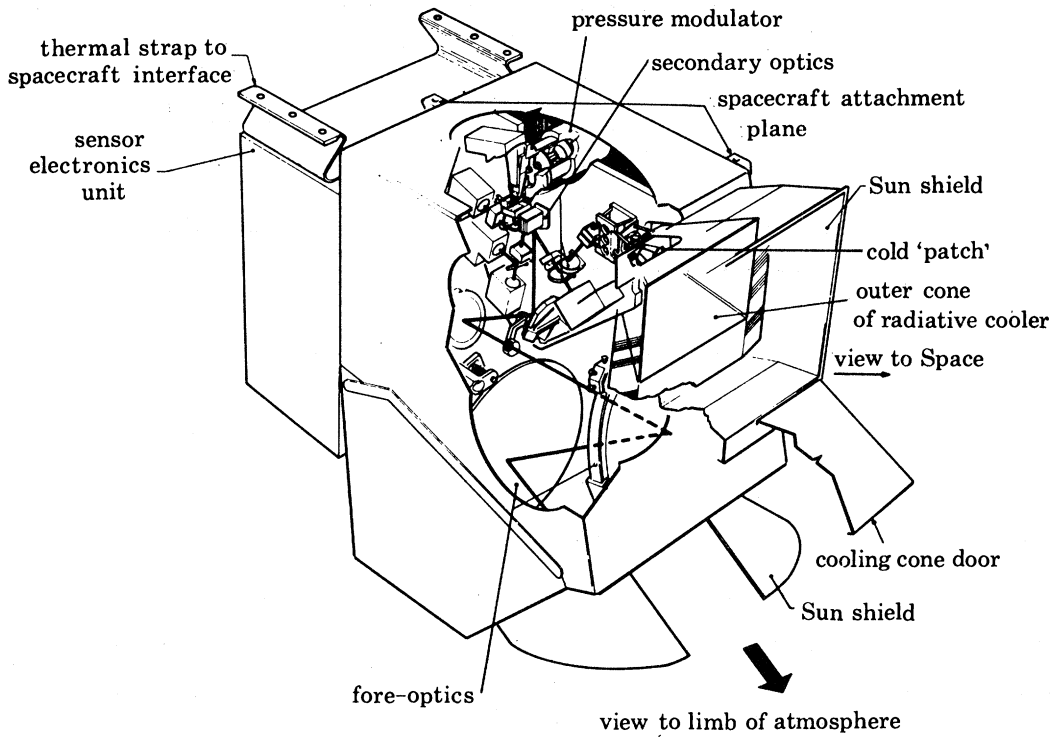

FIGURE 8. Cutaway diagram of the s.a.m.s. sensor unit showing the relative orientation of the optical components, pressure modulators and radiative cooler. The whole unit is located on the sensor ring below the satellite.

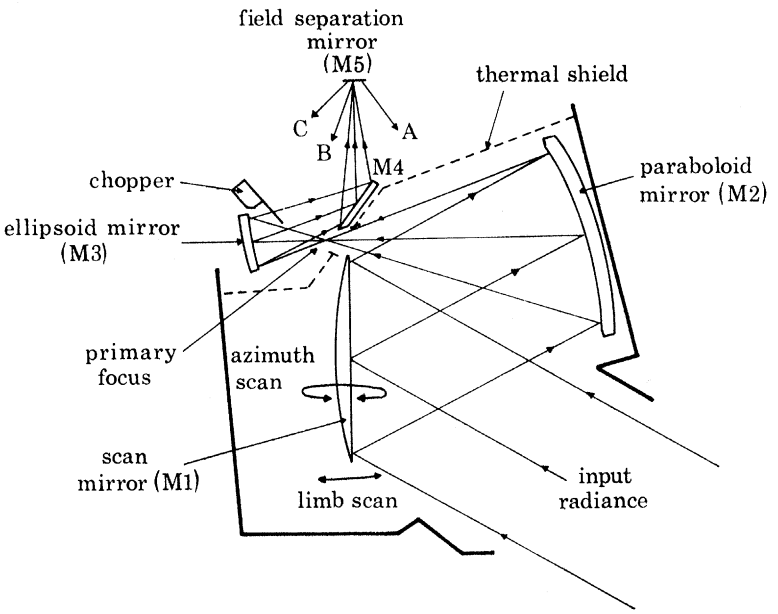

FIGURE 9. The fore-optics of s.a.m.s. in plan view. The calibration black body (not shown) is inserted into the beam at the primary focus. The thermal shield isolates the secondary optics compartment at 25 °C from the front optics compartment at 0 °C.

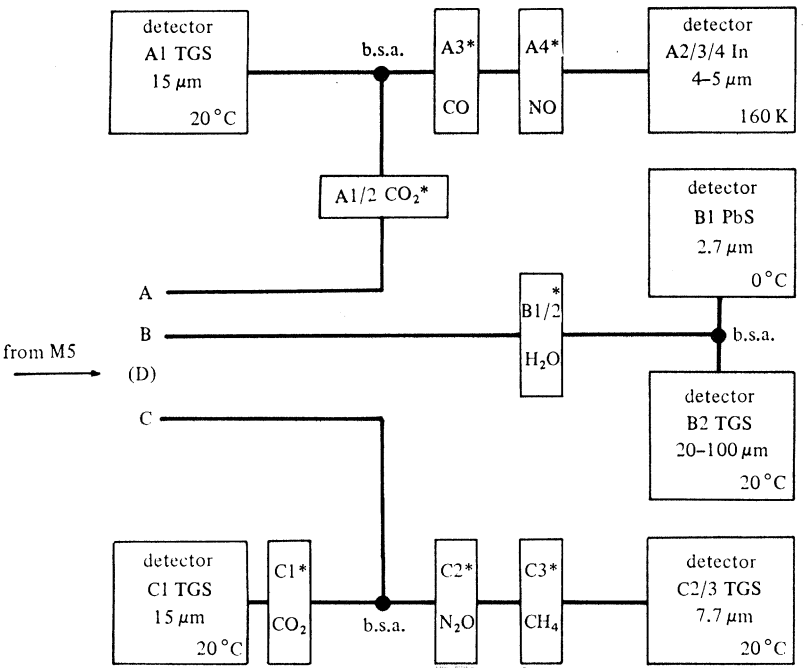

FIGURE 10. Schematic of the secondary optics of s.a.m.s. after the field-separation mirror (M5). The dichroic beamsplitters are marked b.s.A, b.s.B and b.s.C. Secondary mirrors relay lenses and other optical components have been omitted for clarity. The beam marked (D) corresponds to a facet of M5 that reflects the input beam back through the front optics and is used for optical alignment. The pressure modulator cells are identified by an asterisk (*).

PHILOSOPHICAL TRANSACTIONS OF THE ROYAL SOCIETY A MATHEMATICAL, PHYSICAL & ENGINEERING SCIENCES

(M5). The use of an ellipsoid in the M3 position cancels some of the aberrations of the off-axis paraboloid (M2).

Thermal isolation of the compartment containing the first two mirrors, i.e. those before the primary focus and calibration point, allows these mirrors to be run at a somewhat lower temperature (0 °C) than the rest of the instrument, thus reducing the thermal strays from this area and increasing the reliability of the calibration.

The rear optics are shown in the correct spatial orientation in figure 8 and in schematic form in figure 10. Field separation occurs at three of the four facets of the mirror M5 which are angled to direct parts of the beam into one of three separate optical chains, and curved to image M3 on the detector aperture stop. Each of the fields so defined is rectangular and subtends an angle in the instrument line-of-sight $0.16° \times 1.6°$, a solid angle of 7.8×10^{-5} sr (figure 7).

Broad spectral selection for the different molecular bands is achieved by dichroic beamsplitters (b.s.A, b.s.B, b.s.C) and filter packs of up to three separate components on the various detectors. The pressure modulator windows are either anti-reflexion coated or are made of low refractive index materials. In all there are about 40 individual optical components in the system after M5. High optical transmission in the system is maintained by the use of anti-reflexion coatings. As an example, the overall transmission of the C2/3 chain with 19 surfaces is still 67 % at band centre.

The rear optics, modulators and detectors are mechanically and, except for the 2.7 μm PbS and 4–5 μm InSb detectors (B1 and A2/3/4), thermally attached to the main optics plate made of aluminium 1 cm thick giving good thermal uniformity and capacity as well as mechanical stability.

4.2. *Detectors*

There are six detectors in s.a.m.s., four triglycine sulphate (TGS), one lead sulphide (PbS) and one indium antimonide (InSb). Each detector flake is imaged by its optical system on to one of the facets of M5 and, therefore, the aspect ratio of the detectors is the aspect ratio of the field of view. Each detector is 3.12 mm × 0.312 mm, giving an area of approximately 1 mm².

The detectors are each assembled and tested as sub-assemblies consisting of detector, preamplifier, condensing optical system and filters before being integrated with the rest of the instrument. A TGS sub-assembly is shown in figure 11. The condensing optical doublet, consisting of a meniscus and a plano-convex lens (see Murray 1962), is made of anti-reflexion coated germanium (except in the case of the 25–100 μm H_2O channel (B2) where silicon is used). The package consisting of the meniscus lens detector and mounting flange is evacuated to protect the detectors from moisture during ground operations.

The sub-assemblies for the cooled detectors are more complicated than those for the TGS because of the need to isolate the detector thermally while mechanically attaching it to the optics plate. The B1 and A2/3/4 detectors are cooled radiatively, the B1 to 0 °C by a radiator in the fore optics compartment and the A2/3/4 to 160 K by a separate radiative cooler (see § 4.6).

4.3. *Pressure modulator assemblies*

The pressure modulators used in s.a.m.s. are a development of those used in the Nimbus 6 p.m.r. instrument (see Curtis *et al.* 1974). The pressure of the gas in the optical cell is altered by means of a piston oscillating at between 25 and 40 Hz in a connecting volume (figure 12). A pressure variation over the cycle of the order 2:1 is achieved in this design, the exact value depending on the dimensions of the particular optical cell and the mean cell pressure. The principal

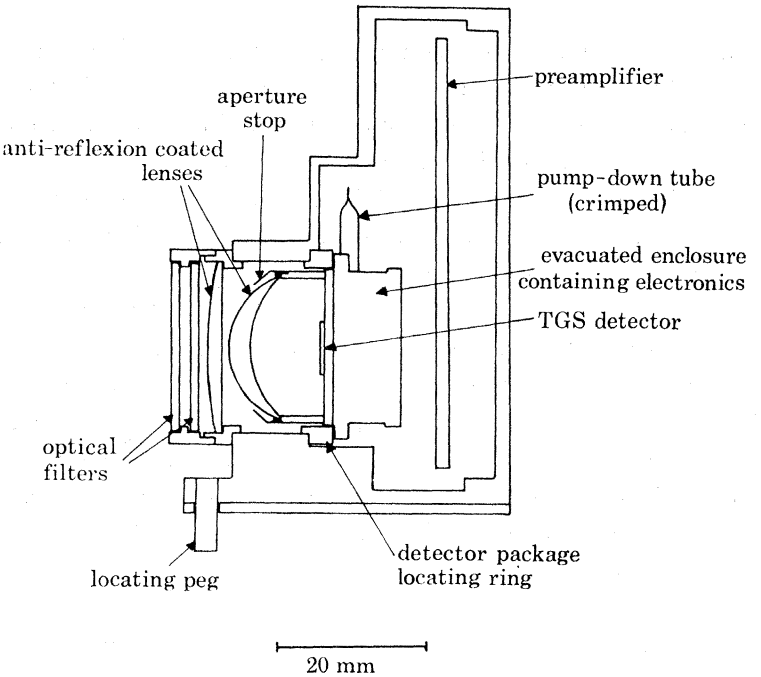

FIGURE 11. S.a.m.s. detector sub-assembly (TGS). Because the impedance of a TGS detector is very high and the signal small, part of the preamplifier is built into the back of the detector package within the evacuated enclosure. Precise optical alignment is essential, both of the package to the sub-assembly and of the sub-assembly to the secondary optics mounting plate. In the former case a close-fitting ring is used and in the latter a precision locating peg.

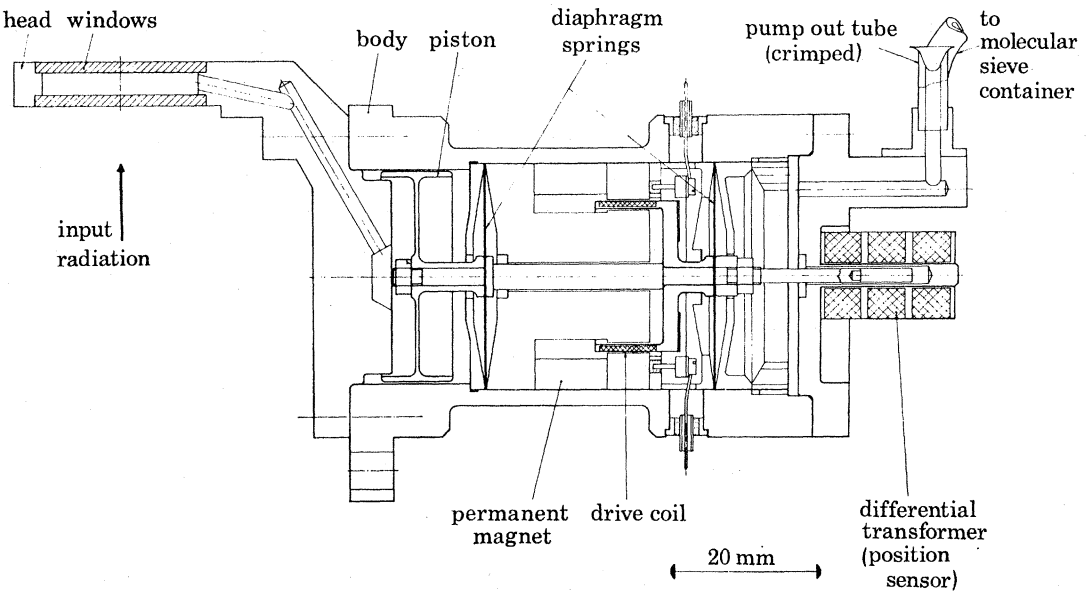

FIGURE 12. Cross section of a p.m.r. assembly. The body of the PMR is made of titanium with gold 'O' ring seals at each end. The support springs and coil lead-outs are made of beryllium–copper. The thermostatted container of molecular sieve is not shown.

changes from the devices used in the Nimbus 6 instrument are a reduction of size by a factor of approximately 2 and the use of a moving coil drive leading to better amplitude control and electrical efficiency. Other improvements have made the modulators easier to manufacture and assemble. It is necessary, as was observed in § 3.2, to alter the pressure of gas in the cell in flight, the pressure selected depending on the altitude range being scanned. This is achieved in the s.a.m.s. modulators as follows. The gas in the cell is in equilibrium with a much larger amount adsorbed on a zeolite molecular sieve material in a reservoir (figure 12). In this system the mean pressure of gas is determined by the temperature of the sieve, and provision has therefore been made for programmable temperature control of the sieve container. Each modulator is provided with two or four pressure settings, which may encompass a range of over 20:1, corresponding to a thermostat temperature range of 30–120 °C. These settings are selected by the program control logic. The adsorption and desorption of gas from the sieve is entirely reversible and the system provides good pressure stabilization. Measurement of the oscillation frequency, which changes rapidly with pressure, is used as the primary method of determining cell pressure since slow variations in gas amount, such as might be caused by a leak in a modulator, could not be detected by monitoring the sieve temperature.

4.4. *Fast chopper assembly*

The fast chopper used on s.a.m.s. only modulates 2.5 % of the beam for reasons described above (see § 2.3). It consists of two etched, black-painted copper grids, mounted one above the other. One grid is fixed to the mount but the other is free to move on the end of a flat cantilever leaf spring. Oscillation, at the mechanical resonant frequency of the spring–grid assembly, is maintained by an electronic loop using redundant pairs of piezoelectric ceramic plates as both drive and position sensors. Oscillation is at a frequency of approximately 245 Hz with a peak-to-peak amplitude of 2 mm.

4.5. *Scan mirror assembly*

The scan mirror must be rotated with high positional accuracy in two mutually perpendicular directions to produce limb and azimuth scanning. This is realized by supporting the mirror in two frames, one within the other, for the two scan directions. Each mirror drive consists of a lead-screw directly driven by a 45° stepping motor. Coupling to the mirror is by means of a recirculating-ball nut, which is lubricated by a lead coating. The axis of rotation of the mirror is defined by a pair of cross-leaf springs (flexipivots). The step sizes of the drive system, expressed in terms of motion of the line-of-sight, are 4.8 arc min in the limb direction and 7.3 arc min in azimuth.

Mirror position is independently sensed in both directions by a linear variable differential transformer (l.v.d.t.), actuated directly by the mirror, and associated electronics. The output of the limb l.v.d.t. is digitized with a resolution of 0.045 arc min and the azimuth l.v.d.t. to 1.8 arc min. It is therefore possible to monitor the limb position of the mirror to a very much higher accuracy than the step size. The limb position is under full control of the program control logic (p.c.l.) (see § 4.7), whereas the azimuth scan can only be programmed as a continuous scan or stepped.

Limit detectors, both optical and mechanical, are provided for resynchronizing the control logic and preventing damage under fault conditions.

4.6. *Radiation cooler*

The indium antimonide detector is cooled by a two stage radiation cooler, the first high-capacity stage forming a cone around the second stage as shown in figure 13. The first stage cools the front lens of the optical doublet (see § 4.2) as well as pre-cooling the rear lens and detector. In orbit, the inner and outer cooler temperatures are typically 160 K and 190 K.

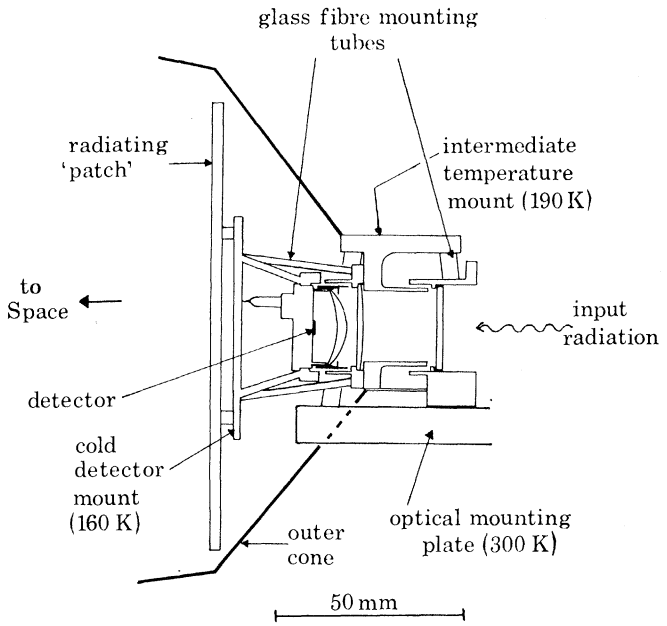

FIGURE 13. The s.a.m.s. cold detector assembly (InSb). The mount is in three parts: the detector mount at 160 K, the intermediate lens mount at 190 K and the mechanical interface at 298 K. The parts are interconnected by 8 glass fibre tubes, some of which may be seen in the diagram. The relative sizes of the 'radiating patch', which is black-painted, and the outer cone, which is coated with vapour deposited aluminium, can be seen in figure 8.

The cooler has been designed to minimize the effects of contamination on the optics as the spacecraft outgases; however, provision has been made to heat the detector and optics electrically to remove the debris as necessary. The cooler surfaces were protected during launch and the first 3 weeks of orbit by a door which was opened on 13 November 1978. The door cannot be closed again and will remain open for the duration of the mission.

4.7. *Electronics*

The electronics of s.a.m.s. is considerably more complicated than that of previous instruments built at Oxford for three reasons:

(*a*) there are more signal channels (twelve in all) and modulator drives (seven);

(*b*) the increased number of signal channels and drives means that more care must be taken to ensure that coupling and cross-talk, both electrical and mechanical, is minimized.

(*c*) The scan and calibration control system is considerably more flexible than previous instruments allowing in-flight programming.

The major changes in construction details since previous instruments are the use of integrated circuit amplifiers in the linear electronics and CMOS in the digital electronics. A full block diagram of the system is shown in figure 14.

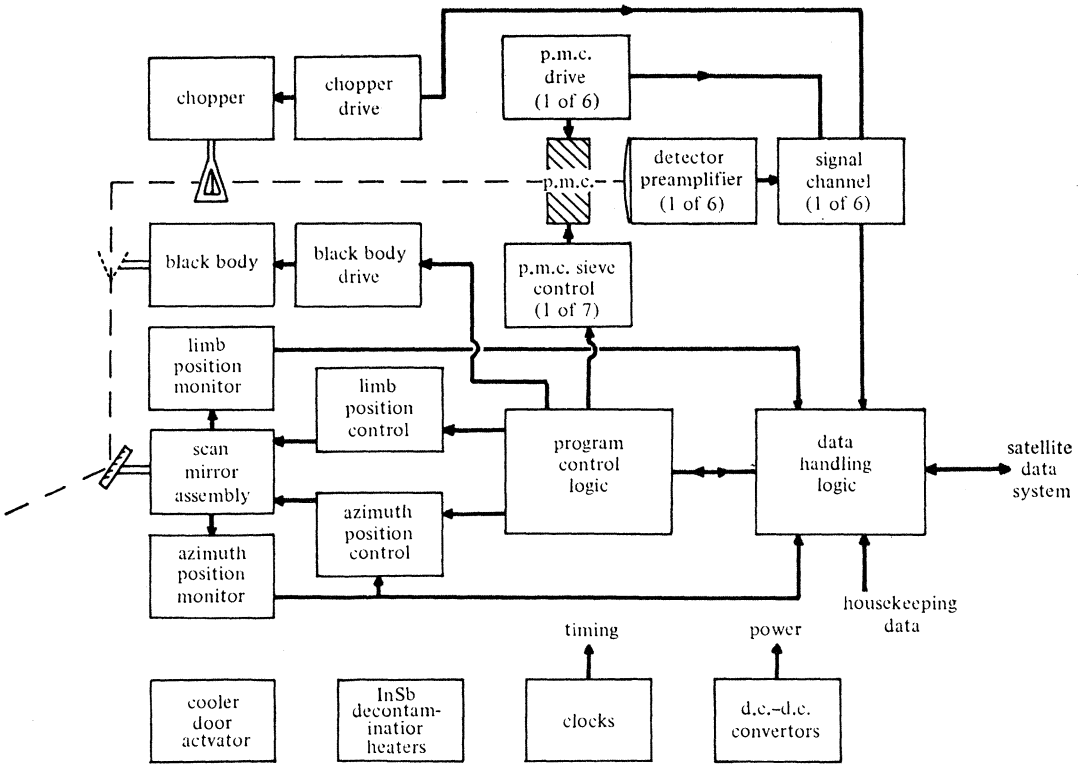

FIGURE 14. Block diagram of the s.a.m.s. electronics subsystems.

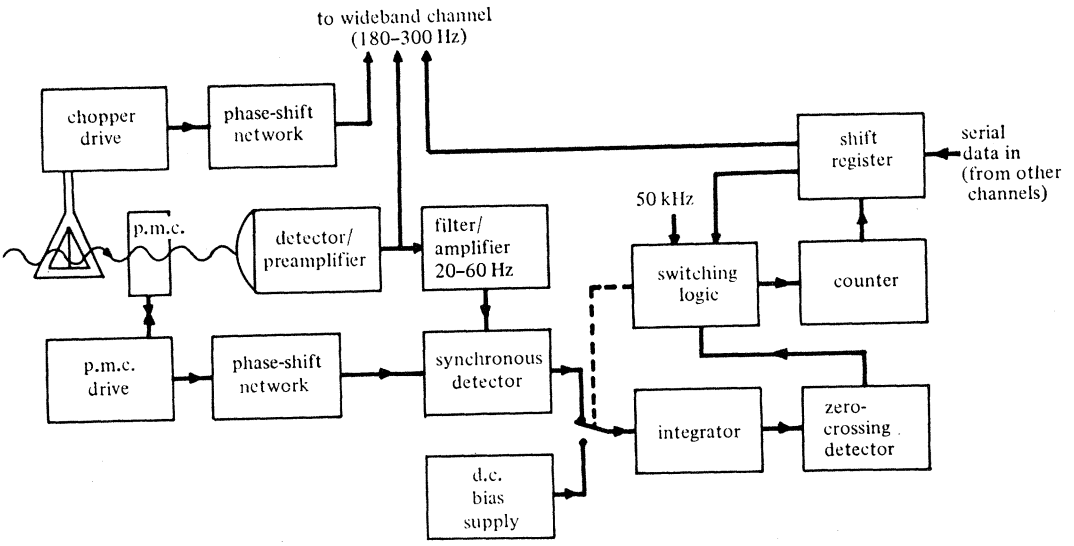

FIGURE 15. Block diagram of one half of a signal channel. Data from all channels is transferred to the data handling system in a single serial stream.

(*a*) *Signal channels*

The signal processing electronics follows the pattern of the system used for a previous balloon radiometer (see Chaloner *et al.* 1978). The high and low frequencies (wideband and pressure modulated signals respectively) present at the detector output are processed by separate channels as shown in the block diagram in figure 15. The output integrator of each channel is also made to act as a dual-slope analogue-to-digital converter. This is achieved by integrating the signal, plus a small offset to ensure that the result is positive, for 1.8 s, and then integrating a fixed negative signal until the result is zero. By timing the second integration period with the use of the 50 kHz spacecraft clock, a resolution of 1 part/10^4 is obtained in the remaining 200 ms of the 2 s period. Only 12 bits are actually telemetred to the ground but the 13th can be inferred, if necessary, by context. The 200 ms period while the signals are evaluated is also used to step the scan mirror.

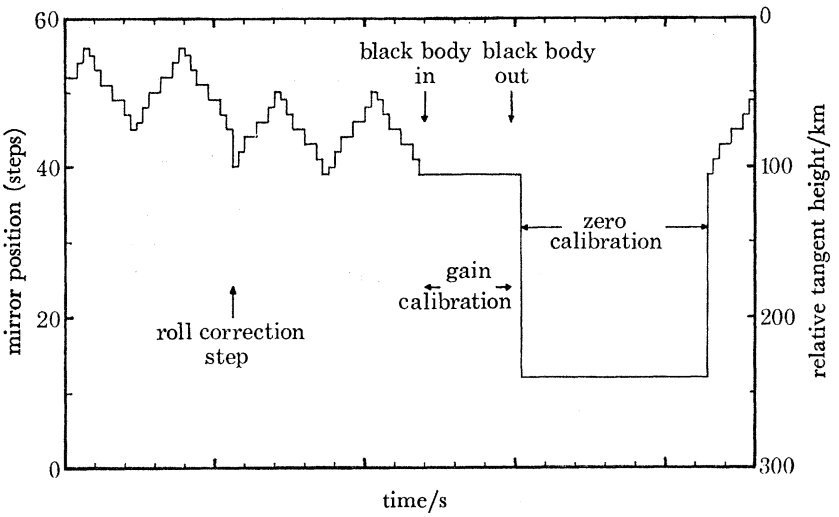

FIGURE 16. A typical scan program. There are 18 scans (up and down ramps) between calibration sequences leading to an interval between calibrations which is not synchronous with the orbital period. Roll correction is applied independently, synchronous with the orbital period.

(*b*) *Pressure modulator drives*

The drive circuits for the pressure modulators are considerably more complex than those used for the Nimbus 6 p.m.r. or the balloon instrument. The complexity is necessary because of the need to maintain a constant amplitude despite large internal pressure variations, which in turn lead to large changes in frequency and power requirements. The use of a moving coil drive, with its inherently tighter coupling than the previous moving magnet drive, assists with amplitude control and also allows active damping to be employed when a modulator is inhibited. Active damping is useful in multiple channels with only one detector (e.g. A2/3/4) since unwanted mechanical energy could otherwise be coupled into the 'off' modulators and appear as unwanted modulation in the detector output. This can be prevented by switching the drive from positive (oscillating) to negative (damping) feedback when the modulator is inhibited.

(*c*) *Program control logic* (*p.c.l.*)

The extremely large number of possible operating modes for s.a.m.s. using various combinations of modulators, scanning ranges and mean cell pressures, and the need to correct the scanning sequences for any predictable orbital roll of the spacecraft, made a programmable operating mode very desirable. The system used operates the scan mirror, modulators, molecular sieves, thermostats and calibration black body by reference to a stored 'program' in a 128×10 bit memory which may be reloaded from the ground. The instruction set of the p.c.l. also includes jump, wait, synchronizing and timing instructions to allow program loops to be constructed which operate in a fixed relationship to the spacecraft data system. The variations of scanning and calibration are, therefore, infinite and it is possible to adapt the scanning sequence to partially compensate for orbital roll. It is also possible to scan outside the atmosphere, for example, to locate the moon for calibration purposes.

A typical scan sequence is shown in figure 16. This program is designed to scan a height range of 55 km in 10 km steps with regular calibration sequences not related to the orbital period. A roll correction step can also be seen.

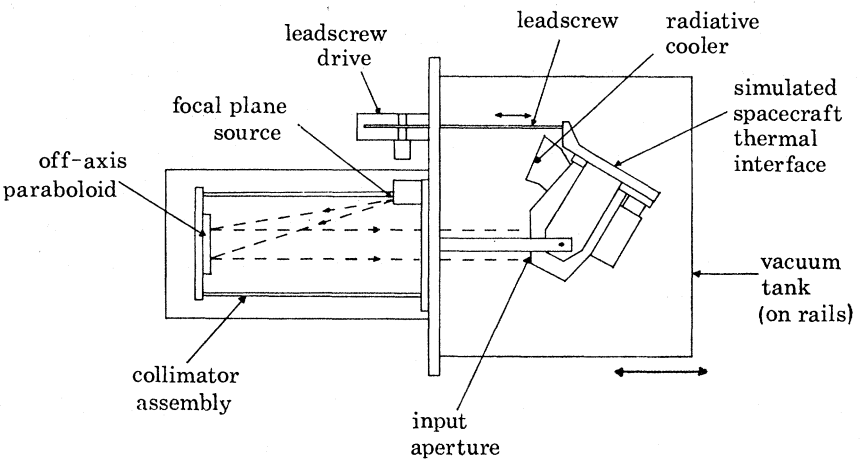

FIGURE 17. S.a.m.s. environmental test chamber at Oxford. Baffles, cooled by liquid nitrogen, surround the instrument to simulate radiative loss to space but these have been omitted for clarity. Access is provided by rolling the main vacuum tank away on rails. The collimator assembly is shown in position. The black body assembly (see text) may be substituted for the collimator when required.

5. VERIFICATION AND CALIBRATION PERFORMANCE

In addition to the tests that were necessary to prove the design of the instrument and the environmental tests specified by N.A.S.A., s.a.m.s. has undergone the following series of measurements intended to facilitate the interpretation of data when in orbit.

(*a*) The response of the instrument to known black body radiance inputs has been measured, and a calibration scheme devised to take account of variations in operating conditions.

(*b*) The response of the instrument to emission from gases in the atmosphere has been determined, using a simulated atmospheric path, in order to verify the spectroscopic calculations by which atmospheric quantities are deduced.

(*c*) The field of view profiles of all the channels and their interrelation has been measured.

(*d*) The scan mirror position telemetry (see § 4.5) has been accurately calibrated in terms of the

instrument line-of-sight. A combined vacuum and thermal environment chamber at Oxford provides correct simulation of the spacecraft interface and orbital conditions. Various additional radiation sources are also available within the chamber for calibration purposes (see figure 17).

5.1. *Radiometric calibration*

The response of the instrument is determined for a range of accurately known black body radiances in order to

(*a*) verify that the instrument response is linear and has the correct gain and noise levels;

(*b*) check that the spectral selection of the optics is correct and that there are no unknown spectral 'leaks' in the overall response;

(*c*) provide a basis for the model of the instrument used in the in-flight calibration scheme;

(*d*) determine the magnitude of any stray responses, particularly those which depend on either azimuth or limb scan angle. The source used for this test is a large, baffled black-body cone, completely filling the instrument aperture, whose temperature may be held constant and uniform at any temperature between 77 K and 320 K. The input radiance is, therefore, very precisely calculable. There are in fact two sources, one on the instrument axis viewed with the azimuth scan centralized and one off-axis viewed at the limit of the azimuth scan. By using both targets, the variations of strays with azimuth scan angle may be established.

Variations with limb-scan angle are measured by tilting the whole instrument using a precision lead-screw, thus varying the relative position of the on-axis target and the instrument.

The sensor temperature is held constant during measurements of stray radiation but may be varied or cycled over a considerable range (-5 to $+40$ °C), in order to dynamically evaluate the temperature coefficients of the response. By simulating the orbital temperature variations of the spacecraft experience is gained of the likely instrument temperature variations in orbit – a verification of the sensor thermal design.

5.2. *Response of p.m. channels to atmospheric paths*

The response of the channels to paths of gas is checked by measurment of the transmission of simulated atmospheric paths in the laboratory, using either the actual sensor modulators, filters and detectors before final assembly of devices identical in design and construction. The apparatus consists of a multiple-pass absorption white cell which provides paths of up to 10 m, which may be used at temperatures down to 240 K (see Houghton & Taylor 1973). Transmissions of isothermal paths of the required absorber or absorber/nitrogen mixtures measured with this equipment as a function of pressure are then compared with the response calculated from line data, and information from both sources is combined in the transmission model used in the final attitude, temperature and composition retrievals.

5.3. *Field of view*

The attitude of the sensor line of sight is determined in orbit from the ratio of the pressure modulator and wideband signals in the CO_2 channels (see § 3.3). The line-of-sight of the other channels, therefore, needs to be measured with respect to these. The details of the field profiles, especially the shape of the lower edge, also critically affect the weighting function of the channels and must also be determined.

For field of view determination the black cones are replaced by a collimator (see figure 17). This consists of an off-axis paraboloid mirror, with a narrow slit illuminated by a hot ceramic

filament in the focal plane. The lead screw system is used to rotate the s.a.m.s. sensor through the parallel beam of radiation from the collimator at a precisely known rate, and the field response is thus determined.

The collimator assembly and leadscrew are also used for various optical checks and in particular for the calibration of the l.v.d.t. system used for limb scan angle telemetry. The lead screw is driven slowly and continuously while the p.c.l. is programmed to step the s.a.m.s. scan mirror so that the edge of the field of view of a selected channel passes through the collimated beam once per step. By matching the respective points on the field response, the l.v.d.t. system is calibrated directly in terms of the line-of-sight. This test and the primary field of view determination are carried out at several temperatures over the desired operating range.

5.4. *In-flight calibration*

A two point calibration is provided in flight as follows.

(*a*) The scan mirror may be programmed to move so that the tangent height viewed in the atmosphere is sufficiently high that the atmospheric radiance is insignificant ('space' view). This is arranged in operational programs such that the minimum tangent height for the lowest field of view (the C channels) is at least 150 km.

(*b*) The black body (see § 4.1) may be placed in the optical path to provide a standard radiance at approximately 295 K. This is also under the control of the p.c.l.

In practice the estimate of the space view signal is much more important than the measurement of gain, as many of the measurements made are of small differences from the zero radiance level. Operational p.c.l. programs are therefore arranged to have a higher proportion of space view calibration than of black body view as shown in figure 16.

In flight the zero offset and radiometric gain are calculated from instrument housekeeping data by means of a model, the parameters of which have been obtained by combining the results of ground tests and in-flight calibration measurements.

6. Preliminary results

Calibrated radiance data from s.a.m.s. is processed in the following sequence. A preliminary estimate is obtained of the tangent pressure of the line-of-sight of all three fields-of-view at all times using the method described in § 3.3. Then the atmospheric temperature profile and a better estimate of the tangent pressure are derived from the preliminary estimate of tangent pressure and the CO_2 channel radiances. Finally, this information is used, together with radiances from the other channels, to retrieve constituent profiles. These three steps are described in some detail below.

6.1. *Attitude determination*

As has already been shown in § 3.3 the tangent pressure of the line-of-sight of the CO_2 channels can be determined from the ratio of the wideband to p.m.r. radiances assuming that the tangent height is within a suitable range (approximately 20–50 km). Since the space-craft roll rate is reasonably low and the orbital period long compared to the rate of sounding (1 every 2 s), smoothing along the orbit path, i.e. in time, is applied using a linear sequential estimator (Kalman–Bucy filtering, see Rodgers 1976). To achieve this the tangent pressure is converted, using a climatological temperature profile and the scan mirror position, to the tangent height of a reference scan mirror position. This tangent height estimate is then smoothed.

The estimator is stepped forwards along the orbit and for each new observation a smoothed estimate of the tangent height and its uncertainty are calculated given the observation and its error, the previous smoothed estimate and its error, the variation in scan mirror position measured by the l.v.d.t., the time between observations and a knowledge of the likely maximum roll rate. The process is repeated backwards along the orbit and the two results at each observation point are combined to derive a best estimate of the roll angle at any point. The smoothed roll-angle is then reconverted to tangent pressure for each field of view. The results for a typical orbit are shown in figure 18.

The smoothing process is capable of dealing automatically with missing data caused either by bad soundings or a tangent height out of the range where attitude determination is possible. Prolonged loss of information produces a steadily increasing uncertainty in the attitude.

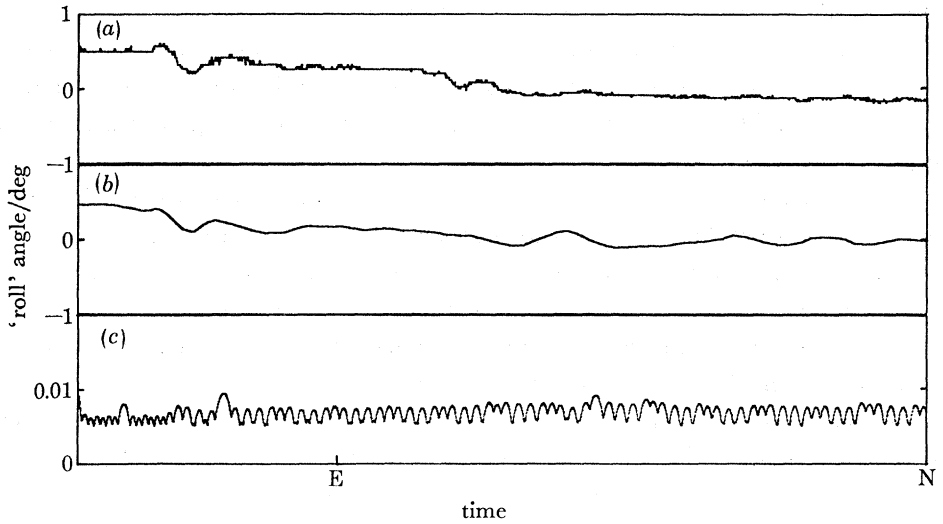

FIGURE 18. A comparison of the 'roll' angle derived as described in the text with the output of the spacecraft attitude control system (for part of orbit 135 of Nimbus 7). For reasons described in the text these are not necessarily comparable but short timescale features should be reproduced. The error in the derived roll error is in a scale magnified 100× relative to the other two plots. E = equator, N = most northerly latitude of orbit. (*a*) Spacecraft attitude control system roll output; (*b*) s.a.m.s. derived 'roll'; (*c*) s.a.m.s. derived 'roll' error.

6.2. *Temperature retrieval*

The short wave channels are particularly sensitive to atmospheric temperature (5 % per degree for the 5 μm channel) so accurate temperature retrievals are of particular importance for making good constituent measurements. It is also possible to improve further upon the attitude determination described above which assumed climatological temperature profiles. Temperature profiles and an improved attitude are, therefore, retrieved simultaneously.

Since there are a large number of possible scan patterns in use, the retrieval method must be able to handle any pattern selected and must, therefore, be very flexible. Were the instrument quickly scanning up and down through the whole atmosphere, complete sets of radiances for a scan could be assembled and the retrieval performed by simpler methods. But there is a need to incorporate observations when and where they occur, essentially at random, and a sequential estimator is again used. For economy of computation the retrieval solution is represented by coefficients of 12 eigenfunctions, giving the deviation of source function at 15 μm from the

climatological mean (interpolated linearly from monthly means at 10° latitude intervals). They are eigenfunctions of the covariance matrix

$$C_{ij} = \exp\left(-(z_i - z_j)^2/\alpha^2\right) \frac{\mathrm{d}B(z_i)}{\mathrm{d}T} \frac{\mathrm{d}B(z_i)}{\mathrm{d}T},$$

where z_i is the scale height of level i and $\mathrm{d}B(z_i)/\mathrm{d}T$ is the differential with respect to temperature at level z_i. This is the Planck function covariance resulting from a set of wave perturbations in

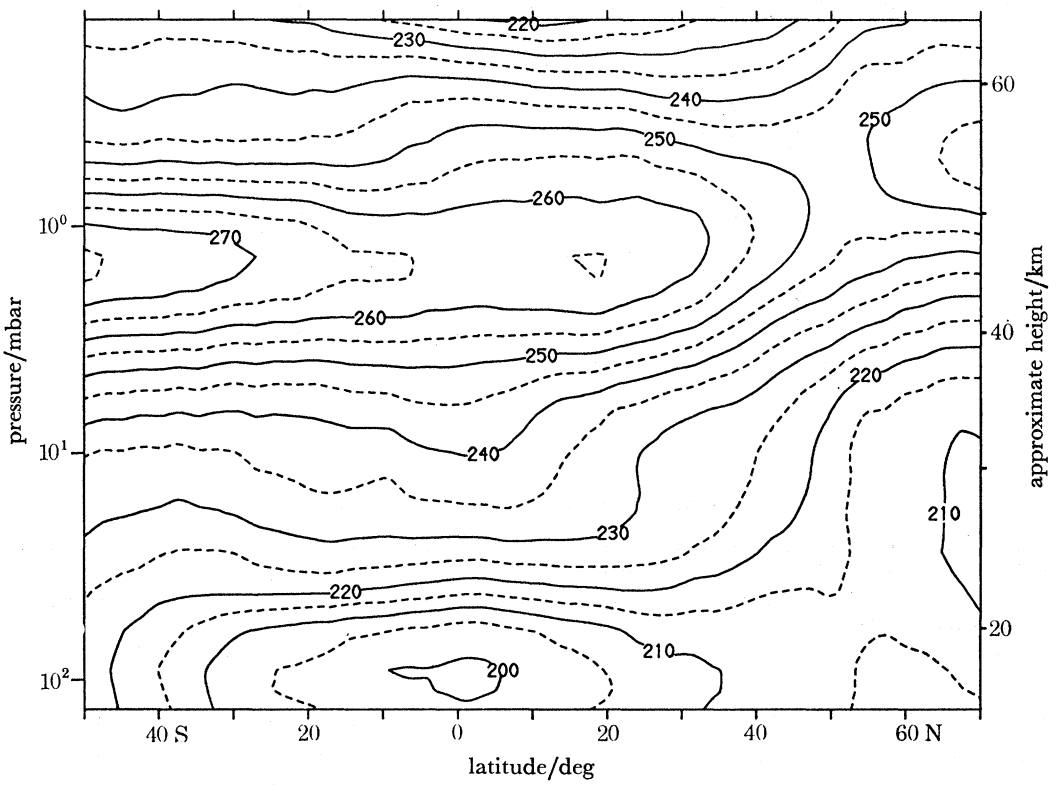

FIGURE 19. Zonal mean temperature cross section for 6 November 1978 derived entirely from Nimbus 7 s.a.m.s. data.

the vertical with a Gaussian spectrum and temperature amplitude independent of height. Using the estimate of attitude derived as above, the deviation of observed radiance from its climatological value can be represented linearly in terms of the solution which consists of the eigenfunction coefficients and the attitude. By these means a linear sequential estimator can be employed in a similar manner to the attitude determination described above. In the absence of input data the solution is made to decay exponentially with time towards zero (i.e. towards its climatological value) so that when there is no information about some or all levels, any deviations for those levels are slowly forgotten. When run forwards along the orbit the estimator is recursive and one-sided, using just past and present data to give the solution. However, an independent set of estimates is obtained by running the estimator backwards along the orbit. At $2\frac{1}{2}$° latitude intervals along the orbit both estimates are combined in accordance with their uncertainties and the result retained for derivation of temperatures and analysis on latitude–longitude grids. A typical zonal mean cross section is shown in figure 19.

6.3. *Concentration retrievals*

Using the derived tangent heights and temperatures it is now possible to obtain concentration profiles from the data. Figure 20 shows some typical results for the H_2O rotation band (channel B2) in both the p.m.r. and wideband cases.

The solid lines were calculated using the temperature data derived using the methods described above, water vapour band data from McClatchey *et al.* (1973) and Chaloner (1976) and a computer program to simulate atmospheric signals due to Eyre (1978).

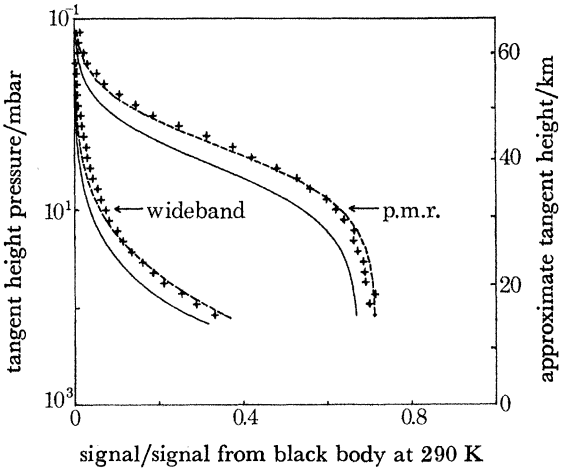

FIGURE 20. Water vapour signal from s.a.m.s. (on 6 November 1978 for latitudes between 20° N and 20° S) compared with signals calculated for constant volume mixing ratio profiles. It can be seen that the p.m.r. signals indicate a slight fall in mixing ratio from 50 to 30 km which becomes pronounced in the wideband signal between 30 and 18 km where there are uncertainties due to clouds and other effects associated with the tropopause. +, S.a.m.s. data; – – –, 5 parts/10^6 by volume; —, 2 parts/10^6 by volume.

Because the data is of a preliminary nature, a profile of concentration versus altitude is not presented. However, it can be seen that the results are inconsistent with a constant mixing ratio profile but would be consistent with a slow rise starting at 20 km levelling off above 35 km. This type of behaviour would be expected if the photolytic destruction of CH_4 were a source of H_2O in the middle stratosphere (McConnell *et al.* 1971).

The project has been supported by the Science Research Council. We particularly acknowledge the invaluable work of the Project Manager, Mr K. H. Davies. Technical support at Oxford was given by Dr P. Curtis, Mr M. Clarke, Mr S. Werrett, Mr M. W. Johnson, Mr I. Colbeck and Mrs C. E. Holt. Substantial assistance in several areas was given by the Rutherford Laboratory, in particular by Mr H. Hadley, Mr J. Parker, Mr R. Wolfenden, Mr G. Stapleton, Mr T. Morgan, Mr R. Elsey and Mr P. Gear. The optical filters and windows were made by Dr J. S. Seeley and Mr R. Hunneman of Reading University. Hawker Siddeley Dynamics (now British Aerospace) at Stevenage built the flight models; we thank in particular Mr G. W. Cocks, Mr J. Bonsor, Mr C. Collins and Mr I. White. Mr W. Andiario has been the experiment representative at the General Electric Company, Valley Forge, during integration of the experiment in the spacecraft. The experiment representative with Nimbus Project, N.A.S.A., was Mr R. White. We gratefully acknowledge the generous cooperation of all members of the Nimbus Project, N.A.S.A.

PHILOSOPHICAL TRANSACTIONS OF THE ROYAL SOCIETY A MATHEMATICAL, PHYSICAL & ENGINEERING SCIENCES

References (Drummond *et al.*)

Chaloner, C. P. 1976 D. Phil. Thesis, University of Oxford.
Chaloner, C. P., Drummond, J. R., Houghton, J. T., Jarnot, R. F. & Roscoe, H. K. 1978 *Proc. R. Soc. Lond.* A **364**, 145–159.
Curtis, P. D., Houghton, J. T., Peskett, G. D. & Rodgers, C. D. 1974 *Proc. R. Soc. Lond.* A **337**, 135–150.
Drummond, J. R. & Jarnot, R. F. 1978 *Proc. R. Soc. Lond.* A **364**, 237–254.
Ellis, P. J., Holah, G., Houghton, J. T., Jones, T. S., Peckham, G., Peskett, G. D., Pick, D. R., Rodgers, C. D., Roscoe, H. K., Sandwell, R., Smith, S. D. & Williamson, E. J. 1973 *Proc. R. Soc. Lond.* A **334**, 149–170.
Eyre, J. R. 1978 D.Phil. Thesis, University of Oxford.
Gille, J. C., Bailey, P., House, F. B., Craig, R. A. & Thomas, J. R. 1975 *The Nimbus* 6 *user's Guide*. Goddard Space Flight Center, Greenbelt, Maryland.
Houghton, J. T. & Smith, S. D. 1970 *Proc. R. Soc. Lond.* A **320**, 23–33.
Houghton, J. T. & Taylor, F. W. 1973 *Rep. Prog. Phys.* **36**, 827–919.
McClatchey, R. A., Benedict, W. S., Clough, S. A., Burch, D. E. & Calfee, R. F. 1973 *A.F.C.R.L. atmospheric absorption line parameters compilation*. AFCRL-TR-73-0096 Environmental Research.
McConnell, J. C., McElroy, M. B. & Wofsy, S. C. 1971 *Nature, Lond.* **223**, 187–188.
Murray, A. E. 1962 *Infrared Phys.* **2**, 37–47.
Rodgers, C. D. 1976 *Rev. Geophys. Space Sci.* **14**, 609–624.
Taylor, F. W., Houghton, J. T., Peskett, G. D., Rodgers, C. D. & Williamson, E. J. 1972 *Appl. Opt.* **11**, 135–141.

PHILOSOPHICAL TRANSACTIONS OF THE ROYAL SOCIETY A MATHEMATICAL, PHYSICAL & ENGINEERING SCIENCES